

Electrical conductivity below 3 K of slightly reduced oxygen-deficient rutile TiO_{2-x}

Ryukiti R. Hasiguti

Faculty of Engineering, The University of Tokyo (Emeritus), Hongo, Bunkyo-ku, Tokyo 113, Japan

Eiichi Yagi

The Institute of Physical and Chemical Research (RIKEN), Wako-shi, Saitama 351-01, Japan

(Received 12 October 1993)

From electrical resistivity and Hall coefficient measurements below 3 K on slightly reduced, semiconductive rutile single crystals with oxygen deficiencies O_d between $3.7 \times 10^{18}/\text{cm}^3$ and $5.5 \times 10^{19}/\text{cm}^3$, it is concluded that the electrical conduction takes place by means of a defect-level permutation conduction mechanism involving Ti interstitial donors. In the range of $3.7 \times 10^{18}/\text{cm}^3 \leq O_d \leq 2 \times 10^{19}/\text{cm}^3$ the electrical resistivity decreases with increasing O_d , while in the range of $2 \times 10^{19}/\text{cm}^3 \leq O_d \leq 5.5 \times 10^{19}/\text{cm}^3$ it increases with increasing O_d . Values of O_d between $8 \times 10^{18}/\text{cm}^3$ and $2 \times 10^{19}/\text{cm}^3$ correspond to the so-called intermediate concentration range of the impurity (defect) conduction, but the transition to metallic-type conduction does not occur because of a change in the defect structures, i.e., the formation of planar defects and the clustering of Ti interstitial donors at higher oxygen deficiencies.

I. INTRODUCTION

Stoichiometric rutile (TiO_2) is an insulator and becomes an n -type semiconductor when it is slightly reduced. This is because lattice defects introduced by reduction act as donor centers. As to the electrical conduction at very low temperatures (below 3 K), it has been proposed that electrical conduction takes place by the defect-related mechanism, i.e., hopping of electrons from lattice defects (donors) to lattice defects (donors),¹⁻⁴ which is similar to the impurity conduction observed in elemental semiconductors like Ge and Si.⁵ Therefore, defect centers play important roles in electrical conduction, especially, at very low temperatures. However, the defect species responsible for this conduction have not been well established.

The defect structures have been extensively studied by various experimental methods, and various types of defects have been reported.⁶⁻²³ It has been also pointed out that the defect structure varies with oxygen deficiency O_d and it is still under discussion which type of defect is dominant in which region of O_d .¹⁸⁻²³ In order to identify defects we have performed experiments using electron paramagnetic resonance (EPR),^{8,9,12} channeling,¹⁷ and transmission electron microscopy (TEM),¹⁴ and obtained rather conclusive direct information as to the identification of several kinds of defects. Therefore, in the present paper we shall discuss the electrical-conduction process below 3 K and the oxygen-deficiency dependence of electrical conductivity in a slightly vacuum-reduced rutile in connection with defect structures.

II. EXPERIMENTAL PROCEDURE

Specimens $12 \times 5 \times 0.8 \text{ mm}^3$ in size were sliced from a stoichiometric Verneuil-grown rutile single-crystal boule of 99.99% nominal purity so that a crystallographic c

axis is parallel to the longest edge and one of a axes is perpendicular to the largest face. EPR experiments made prior to reduction treatment revealed no paramagnetic centers. Specimens doped with Al to the amount of about $6 \times 10^{17}/\text{cm}^3$ with the same orientation were also used.

These specimens were reduced in vacuum by the following method to obtain completely homogeneously reduced specimens. The specimens were sealed in a quartz ampoule, which had been evacuated to about 10^{-5} Torr. After prolonged heating for two weeks at about 1273 K, the capsule was cooled rapidly to room temperature. The amount of oxygen deficiency was estimated by measuring the pressure of oxygen gas, which had developed in the capsule, or the weight loss of the specimen. The specimen with desired oxygen deficiency was obtained by controlling the capsule volume. Such a long heating time to secure completely homogeneous reduction was determined by measuring the electrical resistivities ρ and Hall coefficients R_H as a function of thickness by thinning the specimens, which had been reduced under various conditions. It is to be emphasized here that by preparing these homogeneously reduced specimens the systematic data on the dependence of the electrical conductivity on defect concentration have been obtained.

Although detailed discussion on the conduction above 3 K is not the objective of the present paper, the conductivity data at higher temperatures are highly desirable in order to understand the conduction below 3 K, because, as will be described in Sec. IV, the compensation effect by Al doping and the transition of the conduction, which are reflected in the conductivity data above 3 K, are crucial points for the understanding of the conduction mechanism below 3 K. We have measured these conductivity data, which will also be described in Sec. III.

The reduced specimens were cut into the so-called bridge shape with six side arms for attaching potential leads and Hall leads on both sides of the stem crystal,²⁴

and the measurements of ρ and R_H were made between 2 and 370 K by the conventional method with a vibrating reed electrometer. For the R_H measurements, a magnetic field between 2000 and 3000 G was applied in parallel to the crystallographic a axis.

III. EXPERIMENTAL RESULTS

Figures 1 and 2 show the results of ρ and R_H measurements on the specimens with various O_d between $3.7 \times 10^{18}/\text{cm}^3$ and $5.5 \times 10^{19}/\text{cm}^3$ (or between $\text{TiO}_{1.9999}$ and $\text{TiO}_{1.9983}$). Reduction temperature T_R , O_d , ρ at 2.5 and 300 K, and activation energies are listed in Table I. The R_H curve exhibits two maxima at about 3 K and about 100 K, which divide the temperature region into three, i.e., $T \lesssim 3$ K (region I), $3 \lesssim T \lesssim 100$ K (region II), and $T \gtrsim 100$ K (region III). On the specimens with low oxygen deficiency, conductivities σ can be approximated by a sum of exponentials in regions I and II,

$$\sigma = C_1 \exp(-E_1/kT) + C_2 \exp(-E_2/kT), \quad (1)$$

where E_1 and E_2 represent an activation energy in region I and that in region II, respectively. Excitation of electrons from donor centers to the conduction band is considered to take place in region II.

In region I, R_H decreases with decreasing temperature, while ρ increases gradually. The activation energy E_1 is an order of 10^{-3} eV, which is smaller by a factor of about five than E_2 in region II. They are shown in Fig. 3 as a function of O_d . As shown in Figs. 1 and 2, resistivity decreases over the whole temperature region with increas-

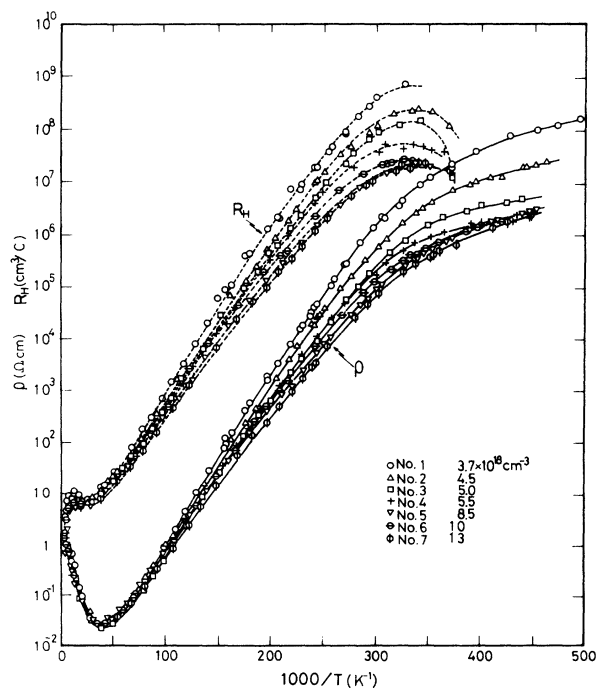


FIG. 1. Electrical resistivities ρ and Hall coefficients R_H of specimens with various oxygen deficiencies O_d between $3.7 \times 10^{18}/\text{cm}^3$ and $13 \times 10^{18}/\text{cm}^3$ as a function of reciprocal temperature $1/T$.

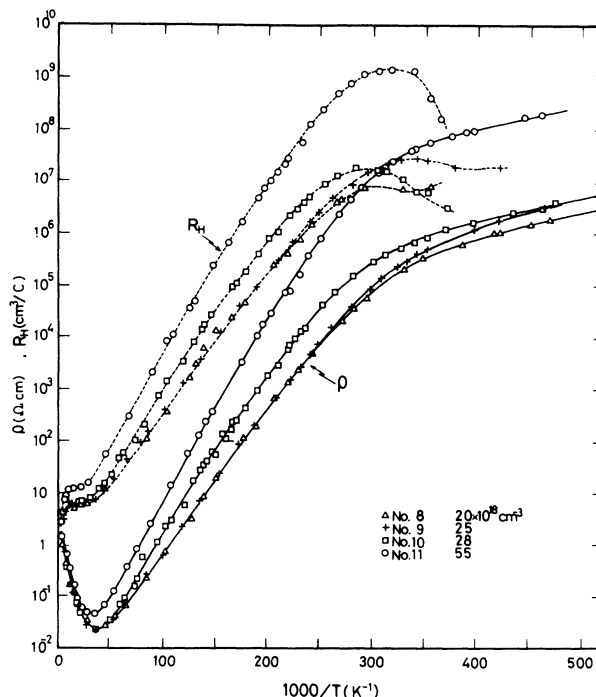


FIG. 2. Electrical resistivities ρ and Hall coefficients R_H of specimens with various oxygen deficiencies O_d between $2.0 \times 10^{19}/\text{cm}^3$ and $5.5 \times 10^{19}/\text{cm}^3$ as a function of reciprocal temperature $1/T$.

ing O_d in the range of $3.7 \times 10^{18}/\text{cm}^3 \leq O_d \leq 2 \times 10^{19}/\text{cm}^3$, while in the range of $2 \times 10^{19}/\text{cm}^3 \leq O_d \leq 5.5 \times 10^{19}/\text{cm}^3$, it increases with increasing O_d . Resistivities at 2.5 K, $\rho_{2.5 \text{ K}}$, are shown in Fig. 4 as a function of O_d together with resistivities at 300 K, $\rho_{300 \text{ K}}$.

In the range $8 \times 10^{18} < O_d \leq 2 \times 10^{19}/\text{cm}^3$, conductivity curves exhibit the deviation from Eq. (1) and have an intermediate slope. They can be approximated by

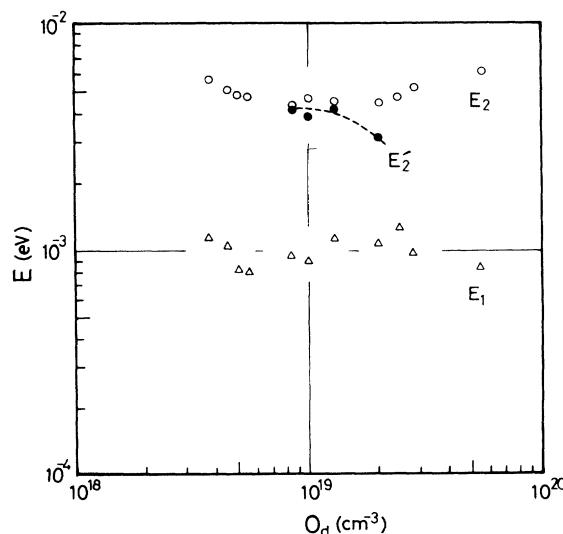


FIG. 3. The activation energies E_1 in region I, and E_2 and E_2' in region II as a function of oxygen deficiency O_d .

TABLE I. Oxygen deficiency O_d , reduction temperature T_R , resistivities at 2.5 K ($\rho_{2.5\text{ K}}$) and 300 K ($\rho_{300\text{ K}}$), and activation energies E_1 , E_2 , and E'_2 .

Specimen no.	O_d (cm^{-3})	T_R (K)	$\rho_{2.5\text{ K}}$ ($\Omega\text{ cm}$)	$\rho_{300\text{ K}}$ ($\Omega\text{ cm}$)	E_1 (eV)	E_2 (eV)	E'_2 (eV)
1	3.7×10^{18}	1273	4.11×10^7	2.48	1.13×10^{-3}	5.57×10^{-3}	
2	4.5	1273	1.12×10^7	1.52	1.03	5.06	
3	5.0	1373	3.20×10^6	1.46	0.81	4.88	
4	5.5	1373	1.84×10^6	1.35	0.76	4.73	
5	8.5	1273	1.58×10^6	0.88	0.98	4.36	4.06×10^{-3}
6	10	1273	1.42×10^6	1.14	0.91	4.79	3.97
7	13	1273	1.15×10^6	1.04	1.15	4.51	4.22
8	20	1273	7.45×10^5	1.06	1.06	4.46	3.19
9	25	1273	1.28×10^6	1.13	1.29	4.73	
10	28	1273	1.63×10^6	1.38	0.98	5.29	
11	55	1273	1.01×10^8	1.65	0.86	6.11	

$$\sigma = C_1 \exp(-E_1/kT) + C_2' \exp(-E_2'/kT) + C_2 \exp(-E_2/kT). \quad (2)$$

The values of E'_2 are also shown in Fig. 3. In the range $O_d < 8 \times 10^{18}/\text{cm}^3$, the low-temperature Hall maximum shifts to higher temperatures as O_d increases, and it becomes almost flat in the range $8 \times 10^{18} < O_d \leq 2 \times 10^{19}/\text{cm}^3$. For $O_d \cong 2 \times 10^{19}/\text{cm}^3$, the R_H curve continues to rise in the temperature region below the low-temperature Hall maximum. This will be discussed in Sec. IV.

Figure 5 shows ρ and R_H curves measured on an un-

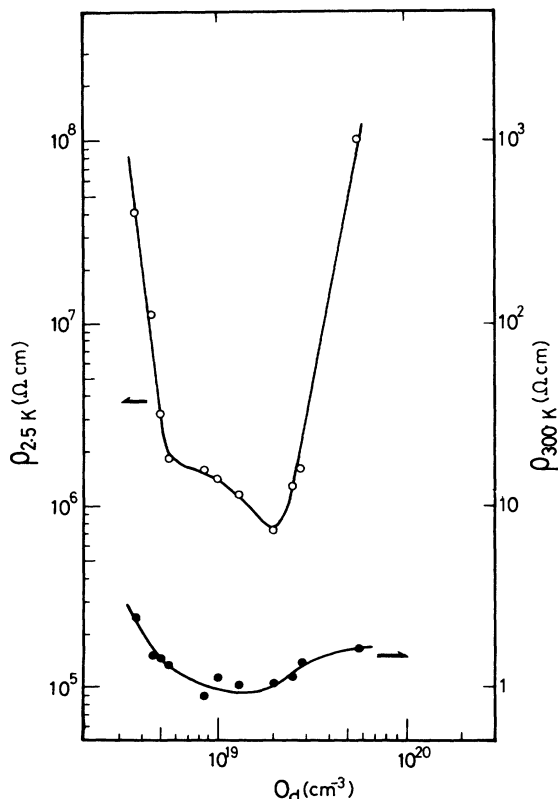


FIG. 4. Electrical resistivities at 2.5 K ($\rho_{2.5\text{ K}}$) and at 300 K ($\rho_{300\text{ K}}$) as a function of oxygen deficiency O_d .

doped specimen and an Al-doped specimen, both of which were reduced simultaneously at 1173 K in the same capsule. Oxygen deficiency was estimated to be about $4 \times 10^{18}/\text{cm}^3$. The doping of Al, which acts as an acceptor, lowered ρ and R_H in region I, whereas it increased them in region II. The activation energy E_1 decreased from 9.5×10^{-4} eV to 8.8×10^{-4} eV by Al doping. A similar effect was also observed by Becker and Hosler.²

On several specimens TEM observation was performed. For $O_d < 2 \times 10^{19}/\text{cm}^3$ planar defects were not observed, indicating that the specimens are in a homogeneous solid-solution phase of point defects. In the specimens with $O_d > 2 \times 10^{19}/\text{cm}^3$, planar defects were observed; $\{101\}$ twin boundaries for $O_d \cong 2.8 \times 10^{19}/\text{cm}^3$

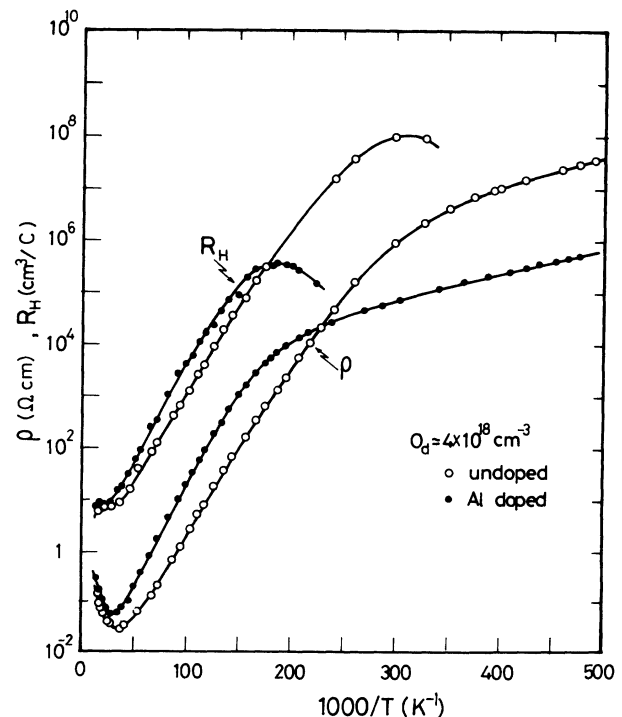


FIG. 5. Electrical resistivities and Hall coefficients of an undoped specimen and an Al-doped one with $O_d \cong 4 \times 10^{18}/\text{cm}^3$.

[Fig. 6(a)] and domain structures having $\{100\}$ and $\{101\}$ boundaries, which are probably antiphase domain structures characterized by the $(\frac{1}{2})\langle 10\bar{1}\rangle$ displacement of adjacent parts across the boundaries, for $O_d \approx 5 \times 10^{19}/\text{cm}^3$ [Fig. 6(b)].

IV. DISCUSSION

Our TEM observations and EPR researches, made also on the same homogeneously reduced specimens, revealed that in the range $O_d < 2 \times 10^{19}/\text{cm}^3$ no planar faults are observed and lattice defects are mostly C centers, the concentration of other kinds of defects being negligible.^{9,12} (The spin concentration in the vertical scale of Fig. 4 in Ref. 9 should be read as an arbitrary unit because of some ambiguity in the calibration of the spin concentration.) According to EPR investigations, the C center was interpreted to be an interstitial Ti ion.^{6-9,12} This interpretation was completely confirmed by our channeling experiments.¹⁷ Therefore, the main defects in

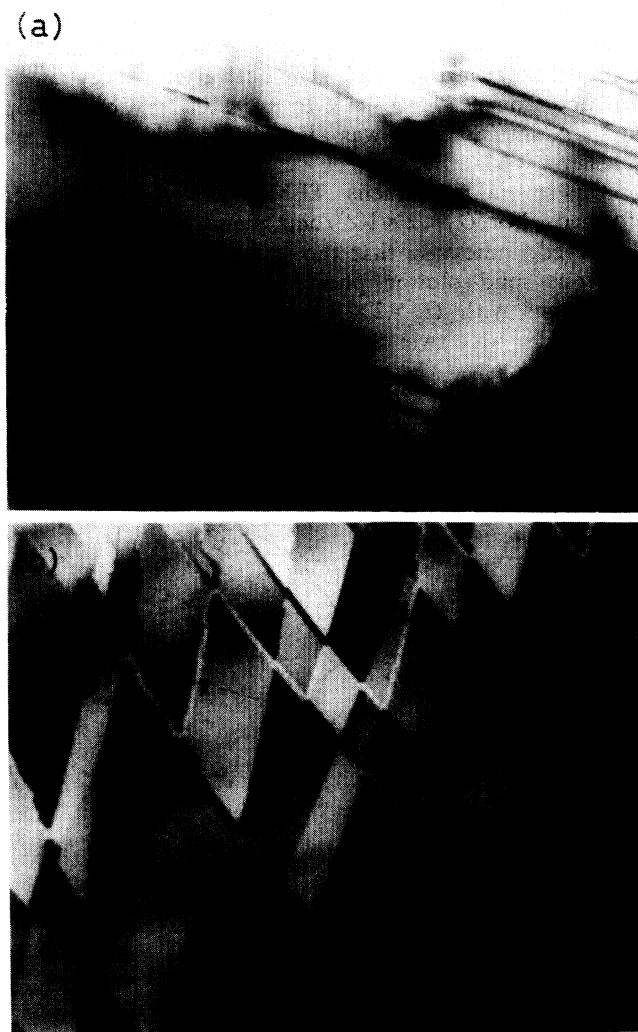


FIG. 6. Electron micrographs obtained on the specimens with (a) $O_d \approx 2.8 \times 10^{19}/\text{cm}^3$ and (b) $O_d \approx 5 \times 10^{19}/\text{cm}^3$. Twin boundaries [in (a)] and antiphase domain structures [in (b)] were observed.

the present specimens with O_d less than $2 \times 10^{19}/\text{cm}^2$ are Ti interstitials. The concentration of C centers increases with increasing O_d ,^{9,12} and, correspondingly, the resistivity decreases as shown in Fig. 1. Hence, the Ti interstitial traps extra electrons and acts as a donor center.

As shown in Fig. 1, at low temperature the R_H curve exhibits a maximum, and in the temperature region below the Hall maximum the resistivity increases slowly with decreasing temperature with an activation energy of about 10^{-3} eV. This behavior is very similar to that observed for the impurity conduction in elemental semiconductors like Ge and Si,^{5,25} and, in addition, the compensation effect by Al doping (Fig. 5) definitely supports a conduction mechanism similar to impurity conduction,^{5,25,26} i.e., hopping of electrons from donors (defects) to donors (defects) (defect-level permutation conduction).

The low-temperature Hall maximum results from the two competing conduction processes, i.e., the defect-level permutation conduction at very low temperatures and band conduction at higher temperatures. The Hall coefficient R_H is expressed as

$$R_H = \frac{n_c \mu_c \mu_{H,c} + n \mu \mu_H}{ec(n_c \mu_c + n \mu)^2}, \quad (3)$$

where n_c , μ_c , and $\mu_{H,c}$ are the concentration of carriers, the drift mobility, and the Hall mobility in the conduction band, and n , μ , and μ_H are the same quantities for the defect-level conduction, respectively. Neglecting any temperature dependence of the mobility, an R_H curve has a maximum at the temperature where $n_c \mu_c = n \mu$. For a specimen with the low donor concentration N_d and the compensation ratio $K (= N_a/N_d, N_a$ is the acceptor concentration) less than 0.5, the mobility μ is given by²⁶

$$\mu = \mu_c n_c / n = (N_d K e \rho_c)^{-1}, \quad (4)$$

where ρ_c is the resistivity at the temperature of the Hall maximum, and the number of carriers n was assumed to be KN_d . From our experiments, it follows that $\mu \approx 2.5 \times 10^{-6}$ cm²/Vs for specimen no. 1 ($O_d \approx 3.7 \times 10^{18}/\text{cm}^3$, $K \approx 0.3$) and $\mu \approx 1.5 \times 10^{-5}$ cm²/Vs for specimen no. 6 ($O_d \approx 10^{19}/\text{cm}^3$, $K \approx 0.25$). In this estimation, it was assumed that $N_d \approx O_d/2$, because donor centers are mostly Ti interstitials. The compensation ratio K was estimated from carrier concentrations in region II using the effective mass, $m^{**} \approx 7m_e$ (m_e is the free-electron mass), which was determined from the temperature dependence of carrier concentrations between 5 and 10 K in the three specimens with O_d of $5 \times 10^{18}/\text{cm}^3$ and less. [A similar value for m^{**} , $(8-10)m_e$, was obtained by Baumard and Gevais.²⁷] The values of K of all specimens lie between 0.2 and 0.4. The mobility μ is very low and characteristic of hopping conduction. Therefore, with the help of our studies on defect structures it is concluded that electrical conduction below 3 K proceeds by the hopping of electrons from Ti interstitials to Ti interstitials.

Now we estimate an effective Bohr radius a_s of a donor electron. According to the results of EPR experiments, the donor center is a Ti interstitial ion where an extra electron is loosely bound. Taking a hydrogenlike model

as a first approximation, a_s is calculated to be

$$a_s = 0.53 \frac{m_e}{m^{**}} \kappa = 7.6 \text{ \AA}, \quad (5)$$

where the effective mass $m^{**} \cong 7m_e$ and the average static dielectric constant $\kappa \cong 100$ ($\kappa_a \cong 89$, $\kappa_c \cong 173$) is used.

From the conductivity in the low-impurity concentration range, Mott and Twose²⁶ calculated the mobility to be independent of temperature and proportional to the square of exchange integral J , e.g.,

$$\mu \propto J^2 = \left[\frac{1}{3} (r_s/a_s)^2 + (r_s/a_s) + 1 \right]^2 \exp(-2r_s/a_s), \quad (6)$$

where r_s is the average impurity center separation (reviewed in Refs. 25 and 26). Kasuya and Koide²⁸ also found that the conductivity is proportional to J^2 . Hence, Ray and Fan²⁵ attempted to fit their experimental data on a p -type Si sample with a simple expression

$$\sigma \propto J^2 \exp(-E_1/kT), \quad (7)$$

and demonstrated that this equation is a reasonable approximation. For their specimens, with a low concentration of impurities, i.e., $a_s/r_s \ll 1$, the data fitted the following equation:

$$\rho \exp(-E_1/kT) \propto J^{-2} \sim \left(\frac{a_s}{r_s} \right)^4 \exp \left(\frac{2r_s}{a_s} \right). \quad (8)$$

The values of $\rho \exp(-E_1/kT)$ were obtained by extrapolating the straight portion of the experimental curve, $\ln \rho$ vs $1/T$, to $1/T=0$. The value of r_s was taken to be $(3/4\pi N_d)^{1/3}$. We shall also try to analyze our data along this line. In Fig. 7, the values of $[\rho \exp(-E_1/kT)]_{1/T \rightarrow 0}$ are plotted against the average donor separation r_s on the

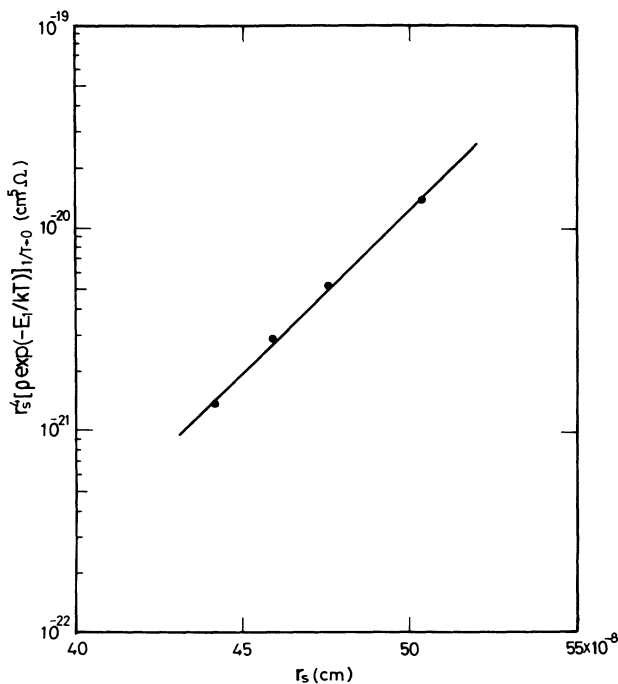


FIG. 7. $r_s^4 [\rho \exp(-E_1/kT)]_{1/T \rightarrow 0}$ as a function of the average donor separation r_s .

four specimens with O_d less than $6 \times 10^{18}/\text{cm}^3$. The following relation was found among them:

$$[\rho \exp(-E_1/kT)]_{1/T \rightarrow 0} \propto \left(\frac{6}{r_s} \right)^4 \exp \left(\frac{2r_s}{6} \right). \quad (9)$$

Hence, $a_s \cong 6 \text{ \AA}$ was obtained. This is in fairly good agreement with 7.6 \AA obtained from Eq. (5).

For impurity conduction in Ge and Si, the transition from the nonmetallic type of hopping conduction to the metallic type of conduction has been observed when the impurity concentration exceeds the critical value.⁵ There exists the intermediate concentration range or the transition range between these two types of conduction. In the intermediate concentration range, the following features were observed.⁵ (i) On the high-temperature side of a Hall maximum, an intermediate slope appears in a curve of $\log_{10} \sigma$ vs $1/T$, the conductivities being approximated by a equation similar to Eq. (2). (ii) A Hall curve has a broad maximum and continues to rise on the low-temperature side of the Hall maximum. In the case of a reduced rutile, such features were observed in the specimens with O_d higher than $8 \times 10^{18}/\text{cm}^3$. Therefore, the oxygen deficiency at the beginning of the intermediate concentration range can be considered to be about $8 \times 10^{18}/\text{cm}^3$, which corresponds to an average donor separation of

$$r_{s,t} = 39 \text{ \AA} \cong 5a_s. \quad (10)$$

This value is not unreasonable if compared with the experimental results that the intermediate concentration range appears at values of $r_{s,t}$ between 2 and $3a_s$ for Sb-doped n -type Ge, and 3 and $4a_s$ for Ga-doped p -type Ge, although they are larger than $2.2a_s$, which was theoretically estimated by Mott for the transition to the metallic type of conduction in the case of hydrogenlike impurities.⁵

The transition to metallic type of conduction does not occur in the present case. The resistivity at 2.5 K increases with increasing O_d for $O_d > 2 \times 10^{19}/\text{cm}^3$ in a similar way as the resistivities at higher temperatures. This is considered to be closely related to a change in the defect structures. For $O_d > 2 \times 10^{19}/\text{cm}^3$, planar defects such as twin boundaries and antiphase boundaries became observed (Fig. 6). For higher O_d , planar defects with $\{312\}$ or $\{725\}$ crystallographic shear structures were observed.¹⁴ EPR experiments indicated qualitatively that around $O_d \cong 1 \times 10^{19}/\text{cm}^3$ the concentration of the C centers begins to decrease, whereas X and W centers appear and their concentrations gradually increase.^{9,12} From the angular dependence of the EPR spectrum, the X center was interpreted to be a Ti interstitial pair.^{9,12} Therefore, Ti interstitials have a tendency to make pairs and further to make higher clusters, which results in the decrease of C centers. The W centers are interpreted to be Ti ion pairs associated with planar defects having crystallographic shear structures characterized by a displacement of approximately $(\frac{1}{2})\langle 10\bar{1} \rangle$. The shear structure having $\{hkl\}$ shear planes like $\{312\}$ and $\{725\}$ are produced as a result of intergrowth of a $\{211\}$ shear struc-

ture and a $\{101\}$ antiphase domain structure so that $\{hkl\} = n\{211\} + m\{101\}$.¹³ Around the $\{211\}$ shear planes, Ti ion pairs are produced,¹⁴ which are the W centers.^{9,12} Therefore, the resistivity increase for $O_d > 2 \times 10^{19}/\text{cm}^3$ is considered to be due to such a change in the defect structures.

V. CONCLUSION

Electrical conduction below 3 K takes place by hopping of electrons among Ti interstitial donors similarly to impurity conduction in Ge and Si. The conductivity of

specimens with O_d between 8×10^{18} and $2 \times 10^{19}/\text{cm}^3$ falls into the intermediate range between hopping and metallic types of conduction, but metallic conduction cannot be achieved at higher O_d because of a change in the defect structures, i.e., the formation of planar defects and the clustering of Ti interstitial donor centers.

ACKNOWLEDGMENTS

The authors thank M. Aono for his help in electrical measurements and S. Takahashi for his help in the specimen preparation.

-
- ¹R. R. Hasiguti, K. Minami, and H. Yonemitsu, *J. Phys. Soc. Jpn.* **16**, 2223 (1961).
- ²J. H. Becker and W. R. Hosler, *Proceedings of the International Conference on Crystal Lattice Defects, Tokyo and Kyoto, 1962* [*J. Phys. Soc. Jpn. Suppl. II* **18**, 152 (1963)].
- ³R. R. Hasiguti, N. Kawamiya, and E. Yagi, *Proceedings of the 7th International Conference on the Physics of Semiconductors, Paris, 1964* (Dunod, Paris, 1965), p. 1225.
- ⁴J. H. Becker and W. R. Hosler, *Phys. Rev.* **137**, A1872 (1965).
- ⁵H. Fritzsche, *J. Phys. Chem. Solids* **6**, 69 (1958).
- ⁶P. F. Chester, *J. Appl. Phys.* **32**, 2233 (1961).
- ⁷P. I. Kingsbury, Jr., W. D. Ohlsen, and O. W. Johnson, *Phys. Rev.* **175**, 1019 (1968).
- ⁸R. R. Hasiguti, E. Iguchi, and S. Takahashi, *Proceedings of the 9th International Conference on the Physics of Semiconductors, Moscow, 1968* (Nauka, Leningrad, 1968), p. 1142.
- ⁹R. R. Hasiguti, *Ann. Rev. Mater. Sci.* **2**, 69 (1972).
- ¹⁰J. Keressen and J. Volger, *Physica* **69**, 535 (1973).
- ¹¹R. R. Hasiguti, in *Proceedings of the International Conference on Radiation Physics of Semiconductors and Related Materials, Tbilisi, USSR, 1979*, edited by G. P. Kekelidze and V. I. Shakhovtsov (Tbilisi State University Press, Tbilisi, 1980), p. 225.
- ¹²M. Aono and R. R. Hasiguti, *Phys. Rev. B* **48**, 12 406 (1993).
- ¹³L. A. Bursill and B. G. Hyde, *Prog. Solid State Chem.* **7**, 177 (1972).
- ¹⁴E. Yagi and R. R. Hasiguti, *J. Phys. Soc. Jpn.* **43**, 1998 (1977); *Lattice Defects in Semiconductors* (Institute of Physics, London, 1974), p. 359.
- ¹⁵L. A. Bursill and M.-G. Blanchin, *J. Phys. Lett.* **44**, L165 (1983).
- ¹⁶L. A. Bursill and M.-G. Blanchin, *J. Solid State Chem.* **51**, 321 (1984).
- ¹⁷E. Yagi, A. Koyama, H. Sakairi, and R. R. Hasiguti, *J. Phys. Soc. Jpn.* **42**, 939 (1977).
- ¹⁸J.-F. Marucco, J. Gautron, and P. Lemasson, *J. Phys. Chem. Solids* **42**, 363 (1981).
- ¹⁹J. Sasaki, N. L. Peterson, and K. Hoshino, *J. Phys. Chem. Solids* **46**, 1267 (1985).
- ²⁰G. M. Raynaud and F. Morin, *J. Phys. Chem. Solids* **46**, 1371 (1985).
- ²¹K. Hoshino, N. L. Peterson, and C. L. Wiley, *J. Phys. Chem. Solids* **46**, 1397 (1985).
- ²²F. Millot, M.-G. Blanchin, R. Tetot, J.-F. Marucco, B. Poumellec, C. Picard, and B. Touzelin, *Prog. Solid State Chem.* **17**, 263 (1987).
- ²³U. Balachandran and N. G. Eror, *J. Mater. Sci.* **23**, 2676 (1988).
- ²⁴P. P. Debye and E. M. Conwell, *Phys. Rev.* **93**, 693 (1954).
- ²⁵R. K. Ray and H. Y. Fan, *Phys. Rev.* **121**, 768 (1961).
- ²⁶N. F. Mott and W. D. Twose, *Adv. Phys.* **10**, 107 (1961).
- ²⁷J. F. Baumard and F. Gevais, *Phys. Rev. B* **15**, 2316 (1977).
- ²⁸T. Kasuya and S. Koide, *J. Phys. Soc. Jpn.* **13**, 1287 (1958).

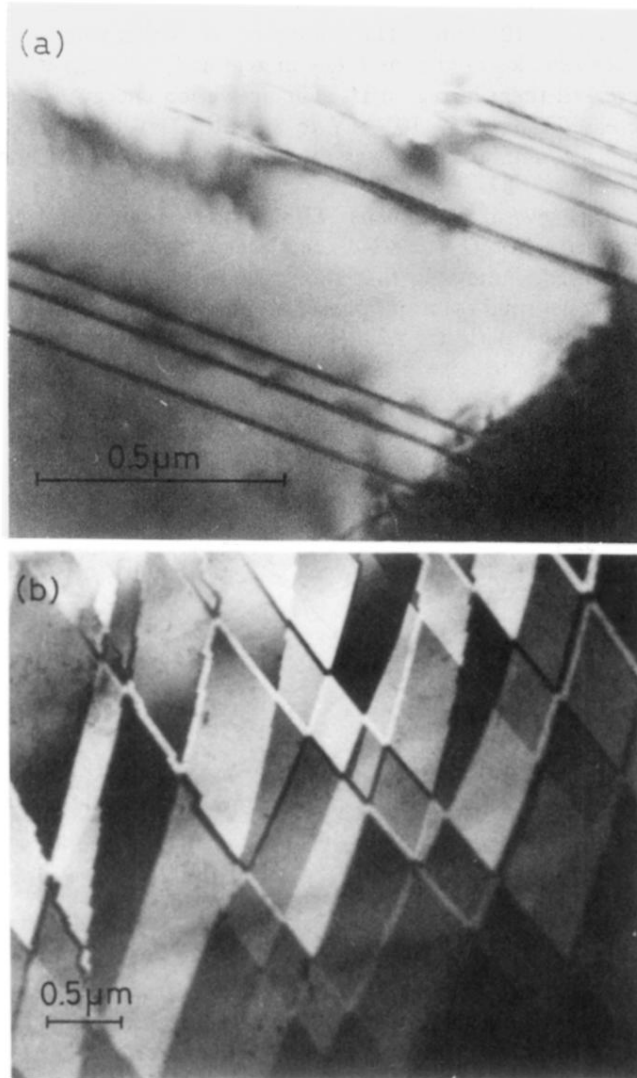


FIG. 6. Electron micrographs obtained on the specimens with (a) $O_d \cong 2.8 \times 10^{19}/\text{cm}^3$ and (b) $O_d \cong 5 \times 10^{19}/\text{cm}^3$. Twin boundaries [in (a)] and antiphase domain structures [in (b)] were observed.